Journal of
Water & Climate Change

IWA PUBLISHING

Journal of Water and Climate Change Vol 15 No 2, 733 doi: 10.2166/wcc.2024.550

Energy-based hydro-economic modeling of climate change effects on the Upper Euphrates Basin

Ayca Aytac [a,*], Mustafa Sahin Dogan [b] and M. Cihat Tuna [c]

[a] Department of Civil Engineering, Dogus University – Dudullu Campus, Istanbul, Turkey
[b] Department of Civil Engineering, Faculty of Engineering, Aksaray University, Aksaray, Turkey
[c] Department of Civil Engineering, Firat University, Elazig, Turkey
*Corresponding author. E-mail: aaytac@dogus.edu.tr

AA, 0000-0002-2108-6363; MSD, 0000-0002-3378-9955; MCT, 0000-0001-9005-1968

ABSTRACT

Climate change and global warming are expected to affect water resources management and planning, requiring adaptations to changing conditions. Therefore, it is very important, especially for decision-makers, to identify demand deficits due to less water availability with climate change that may occur in the existing water supply system in advance. FEHEM, a hydroeconomic optimization model of the integrated reservoir system of the Upper Euphrates Basin, which is the largest and main basin providing water flow to the Euphrates River, is developed. Using a 45-year historical hydrological dataset, water management and hydroelectric operations are evaluated with a linear programming model at monthly time steps. The effects of climate change on the Upper Euphrates Basin are evaluated under low and high carbon emission scenarios. According to the average of the different climate scenarios studied in the model, the average decrease in flows is 37.5%. With climate change, peak flows will occur about 1–2 months earlier on average. As a result of these hydrological changes, the total amount of energy production in the basin will decrease by about 54% and energy revenue by the same percentage.

Key words: climate change, FEHEM, hydroelectric generation, optimization model

HIGHLIGHTS

- Two climate scenarios, one with high and the other with low emissions, were studied in the Upper Euphrates Basin. In both scenarios, there was a 37.5% reduction in flows on average.
- Moreover, the production of 10 large storage hydroelectric power plants in the Upper Euphrates Basin will decrease by approximately 50% according to different climate scenarios.
- The break in energy income in the basin caused by climate change was calculated.

1. INTRODUCTION

Climate change brings significant changes in long-term weather patterns and is being felt more intensely today due to the increase in anthropogenic activities. Most of this observed global warming is due to human activities. Recent climate simulations show that if emissions of carbon dioxide and other greenhouse gases continue to rise, the global annual average temperature will rise by 2.5–4 °C by the end of the 21st century. Global warming due to increased greenhouse gas emissions has led to changes in the distribution of water resources in many regions of the world, and global and regional hydrological cycles have been greatly affected (Solomon *et al.* 2007; Dufresne *et al.* 2013; Hagemann *et al.* 2013).

Climate change over the basins of Turkey has been evaluated in several studies with various aspects. Different hydrological scenarios are used to determine the effects of climate change in projection studies for the optimum operation of reservoirs (Zaman *et al.* 2016; Farjad *et al.* 2017; Morid *et al.* 2019). Prior research has also highlighted many economic elements of water resource management, including optimizing job prospects while considering water allocation optimization (Davijani *et al.* 2016). Sustainable agriculture can be achieved by using water resources as efficiently as possible (Tian *et al.* 2018). Agriculture water management also requires economic optimization (Zhang & Guo 2016). Recent research has combined the economic and environmental components of global warming. These studies presented a creative framework to measure

the harmful effects of global warming, with climate change-related water decisions at a local scale connected to the river basin economy (Auffhammer 2018; Eamen *et al.* 2021).

Investigating the geometric and topological properties of river networks is important for developing predictive models describing the network dynamics under changing climate as well as for quantifying the physical processes operating upon them (Sarker 2020). Various components of the climate change impact studies have been reviewed in the literature. Galavi *et al.* (2023) analyzed the possible impacts of climate change on the river flow of the Hulu Langat basin. Galavi & Mirzaei (2020) analyzed the possible impacts of climate change on the river flow of the Sarbaz River Basin and the tropical Hulu Langat River Basin.

Climate projections show that temperature will have increased by the end of the current century. Nearly all of these projections indicate that precipitation will decrease significantly in Southern Europe and the Mediterranean Basins, including the Upper Euphrates (https://www.tarimorman.gov.tr/).

The high- and low-emission climate scenarios used in this study represent an increase in air temperature and a decrease in rainfall. These future changes are likely to have a major impact on high-bodied hydroelectric facilities, especially those with low storage capacity. According to the scenarios, precipitation is more likely to be in the form of rain and lead to temporally earlier snowmelt. This will lead to disruption of flow regimes and large flows in shorter time periods. Reservoirs with low storage capacity will not be able to store this water and will have to spill excess water, resulting in an economic loss. However, hydroelectric plants with large storage capacities will be able to store large flows that will arrive at earlier times and adapt more easily to these climatic changes. Therefore, hydroelectric plants with large storage capacities will be less affected with adaptations. Especially in the summer months when energy demand is high, reduced flows due to climate change will decrease hydroelectric power generation and this will negatively affect the energy market. Reduced energy production will lead to higher energy prices (Dogan 2015).

According to international figures, hydropower generates 70% of all renewable electricity and about 16% of the world's total electricity (Feng *et al.* 2018). Due to its many benefits, including its exceptionally low cost and lack of greenhouse gas emissions, hydropower generation is one of the most popular ways to produce electricity in the world. It is therefore crucial to assess how susceptible hydropower systems are to climate change consequences (Jakimavičius *et al.* 2020). Due to what appears to be climate change, concern over the management and use of water resources has increased in recent decades (Xu *et al.* 2020).

Many studies have examined how hydropower generation changes as a result of climate variations, including Ye *et al.* 2020; Yu *et al.* 2020; Di Piazza *et al.* 2021; and Garrido-Perez *et al.* 2021.

The FEHEM is a hydroeconomic optimization model for the interconnected water supply system of the Upper Euphrates Basin. The FEHEM represents approximately 8.1% of Turkey's total drainage area. Using 45 years of historical hydrological data to represent hydrological variability, the model determines the optimum hydropower generation decisions of the modeled reservoirs. Using the developed model, it will be possible to prepare water management plans under different policies and future climate scenarios to determine adaptation strategies in advance (Aytac *et al.* 2023).

In this study, hydroelectric modeling of 10 reservoirs in the study area under different climate scenarios is carried out. Reservoir storage capacities range from 0.23 to 295 billion cubic meter (BCM) with power capacities from 50 to 1,330 megawatts (MW). The linear programming (LP) method is selected due to its advantages, such as fast calculation and guaranteed feasible optimal solution, in large-scale reservoir system modeling (Dogan *et al.* 2021). In the LP hydroelectric optimization model, two different scenarios with high emissions and low emissions are studied by perturbing 45 years of historical hydrological data. Reservoir storage, release, hydroelectric generation, revenue, and capacity factor results under climate change are evaluated and compared to historical hydrology.

2. MATERIALS AND METHODS

2.1. Study area

The Upper Euphrates Basin is one of the largest basins in the eastern region of Turkey. It is the richest region of the Middle East in terms of water resources. The map showing the basins, rivers, and dams in the study area is presented in Figure 1.

In the model study covering such an important region, the monthly flow time-series of Karasu River, Murat River, Munzur Stream, and Peri Stream between 1971 and 2016 are considered. These rivers and streams combine to form the Euphrates River. The network representation of the modeled tributaries forming the Euphrates River is presented in Figure 2.

Figure 1 | FEHEM study area.

All rivers in the study area show typical snow-fed river characteristics. Significant melting in the rivers starts mostly in March and ends in June and July. Most of the peaks, which are a significant portion of the annual discharge, occur in April and May. Many large hydroelectric facilities have been built to generate energy from the rich water resources in the region.

The Upper Euphrates Basin hydroelectric facilities account for about 20% of Turkey's total hydroelectric power generation, depending on the hydrological variability. General information about the hydroelectric facilities in the Upper Euphrates Basin is given in Table 1. Half of the hydroelectric energy of the Upper Euphrates Basin comes from the 1,330 MW Keban Dam on the main tributary and the rest from the Murat, Peri, Karasu, and Munzur River energy levels. Power generation in the basin is mostly done with water from snowmelt (often stored).

2.2. Climate scenarios and GCMs climate models

The general circulation of the planet's seas and atmosphere is simulated by the global circulation model (GCM). General circulation refers to large-scale atmospheric or oceanic motions that can have both persistent and cyclical characteristics. The

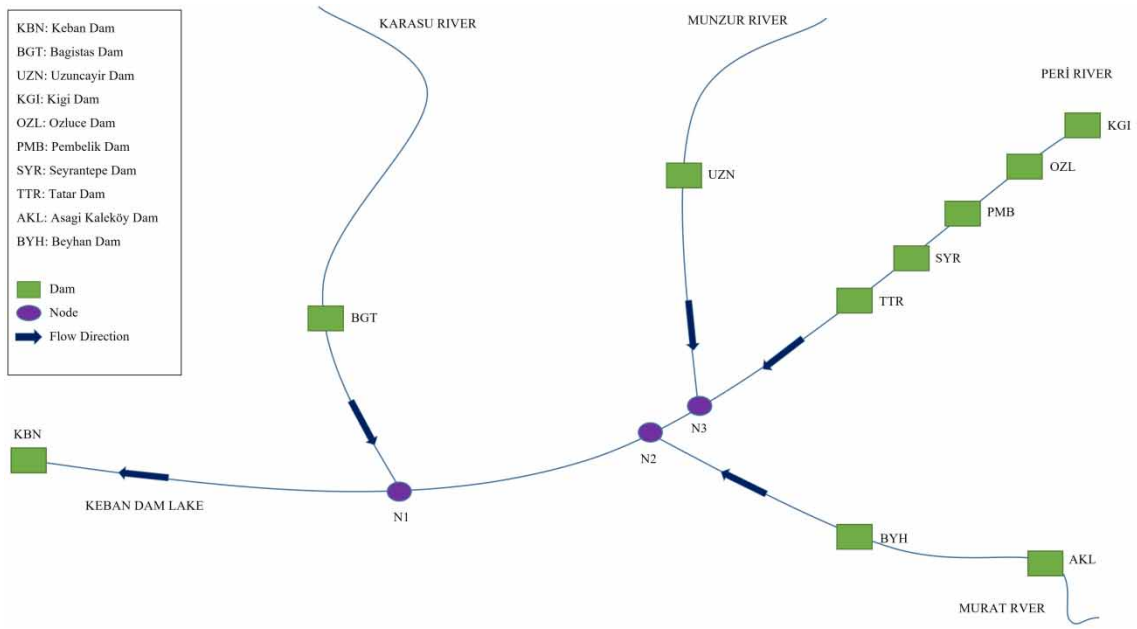

Figure 2 | FEHEM model network representation (Aytac *et al.* 2023).

Table 1 | The Upper Euphrates Basin hydroelectric facilities

Dam ID	Dam name	Installed capacity (MW)	Turbine flow (m^3/s)	Max. water level volume (hm^3)	Lake area (km^2)	Net head (m)	Tailwater elevation (m)
Bagistas	BGT	140.63	351.57	250.00	15.58	50.00	862.00
Uzuncayır	UZN	81.99	157.67	307.93	13.43	65.00	845.00
Kigi	KGI	138.00	104.54	507.55	8.40	165.00	1,225.00
Ozluce	OZL	170.00	147.56	1,081.5	25.80	144.00	1,020.00
Pembelik	PMB	127.34	212.23	358.38	15.63	75.00	954.00
Seyrantepe	SYR	56.84	197.36	24.01	1.50	36.00	920.00
Tatar	TTR	128.22	228.96	299.57	13.07	70.00	848.00
Beyhan	BYH	582.10	868.70	590.98	19.15	76.00	903.00
Asagi Kalekoy	AKL	500.00	628.73	596.06	15.90	87.55	1,012.00
Keban	KBN	1,330.00	1,146.55	29,764.60	687.00	145.00	692.00

GCM uses both empirical computations to duplicate processes based on data and mathematical formulas to represent the controlling physics of circulation processes.

Because of these characteristics, general circulation models are the main tools for generating climate change projections based on emission scenarios. These projections are widely used to study the impacts of climate change on different components of the climate system at global and continental scales (Russel *et al.* 2000).

Hydrologic effects of future climate change in the basin have been investigated using dynamically downscaled outputs of different GCM (ECHAM5 and CCSM3) simulations via a regional climate model (RegCM3), obtained from a PhD thesis entitled with 'Climate Change Impacts on the Hydrology of the Euphrates-Tigris Basin' (Bozkurt 2013). In the same study, in addition to the analysis of atmospheric model outputs, the impacts of future climate changes on river discharges in the basin were investigated via a hydrological discharge model (the HDM). Hydrological discharge simulations were carried out using surface runoff and drainage outputs of CMIP3 simulations of ECHAM5. In addition to this, the HDM was forced by high resolution regional climate model outputs of different GCM-emissions simulations under ECHAM5 and CCSM3 scenarios.

The current measurement values using CCSM3 with high carbon emission and ECHAM5 with low-emission simulations (CMIP3 models RCP 4.5) for 1960–2016 of Palu and Bagistas observation stations, which represent the flows of the Upper Euphrates Basin, were compared with the flows for 2070–2100 which were obtained from climate model simulations. Percentage differences between them according to months were determined.

All of the historical data used in the manuscript are actual observational data taken from nearly 100 current observation stations in the study area. The FEHEM model uses historical hydrology to represent the hydrologic variability. The base historical case uses historical observed data. For climate change runs, the historical hydrology is perturbed with inflow multipliers to reflect climate change.

Operations under CCSM3 and ECHAM5 climate scenarios are evaluated, in addition to historical climate. The use of both climate models is justified due to their widespread use in scientific studies, international acceptance within the scientific community, and their open-source code. When reviewing the literature, it is evident that all climate models predict a decrease in precipitation and an increase in temperature in the future. Consequently, a common projection among all climate models is a decrease in streamflow. Therefore, regardless of the climate model, the hydroeconomic situation in the Euphrates Basin has been projected in the near future, considering a decrease in streamflow.

2.2.1. CCSM3 climate model

The community climate system model (CCSM) is a unified model for simulating past, present, and future climates. In its current form, the CCSM consists of four components for the atmosphere, ocean, sea ice, and land surface, connected through a coupler that exchanges flow and state information between these components (Collins *et al.* 2006). It is developed and used by an international community of scientists from universities, national laboratories, and other relevant institutions. In this study, simulation values with CCSM3 high-emission scenario are used.

2.2.2. ECHAM5 climate model

The fifth-generation atmospheric general circulation model (ECHAM5), developed at the Max Planck Institute for Meteorology, is the latest version of a series of ECHAM models that originally evolved from the spectral weather prediction model of the European Center for Medium-Range Weather Forecasts. It describes the dynamics of the Earth's atmosphere, including physical, chemical, and biological processes and especially the contributions of human behavior. Simulations with ECHAM5 are part of the Earth system research that strategically aims to predict climate dynamics. The ECHAM source code is generally available free of charge (Roeckner *et al.* 2004). ECHAM5 low-emission scenario simulation values are used in the study.

2.3. Model development

Hydrological and economic data are used in hydroeconomic optimization models. Hydrological data consist of reservoir and tributary flows and evaporation rates. Reservoir storage capacities and hydroelectric turbine capacities also constitute the model inputs. Economic data consist of unit operating costs and unit energy prices. The main model outputs are reservoir water storage and releases, hydroelectric energy production, and revenue.

The FEHEM model, a deterministic hydroeconomic optimization model of the Upper Euphrates Basin, is an adaptation of the CALVIN (California Value Integrated Network) model. CALVIN is a hydroeconomic optimization model for California's interconnected water supply system (Draper *et al.* 2003; Dogan *et al.* 2018). FEHEM uses a network-flow structure and is modeled using Pyomo, a Python-based high-level optimization modeling language (Hart *et al.* 2017). In network-flow problems, the physical system is represented by a set or matrix of nodes (N) and a set of links (A). In hydroeconomic optimization models, where the objective is to minimize operating costs and maximize hydroelectric generation revenue, this process can be expressed mathematically by the following objective function:

$$\min z = \sum_i \sum_j \sum_k c_{ijk} X_{ijk}, \quad \forall (i, j, k) \in A \tag{1}$$

In Equation (1), z represents the cumulative cost. For each link, index i represents the start node and index j represents the end node. In the piecewise LP technique, k represents each linear segment. The k part is resulted from the linearization of nonlinear cost functions and c represents the linear unit cost. In this equation, the independent variable is X and represents the flow from node i to node j. All functions used in the model must be convex in minimization problems to guarantee global optimum. For hydroelectric modeling, the inverse of the benefit curve (penalty) is taken to maximize hydroelectric generation.

$$x_{ijk} \geq l_{ijk}, \quad \forall (i, j, k) \in A \tag{2}$$

$$x_{ijk} \leq u_{ijk}, \quad \forall (i, j, k) \in A \tag{3}$$

$$\sum_i \sum_k X_{jik} - \sum_i \sum_k a_{ijk} X_{ijk} = 0, \quad \forall (i, j, k) \in A \tag{4}$$

Equation (1) is subject to three constraints. The first limiter represents the lower flow limit (l) for each link (Equation (2)). This lower limit can also be used to represent minimum flow requirements. The second limiting function (Equation (3)) represents the upper limit (u) on a given link. This function can also be used to represent the capacity for reservoirs, canals, and turbines. The last limiter (Equation (4)) represents the mass balance. For each connection, the incoming flow must be equal to the outgoing flow. In this function, a is used to represent loss factors such as evaporation. All parameters (c, l, u, and a) are predetermined and fixed.

The objective of the FEHEM model is to minimize costs and maximize hydroelectric generation. All equations expressed mathematically in Equations (1)–(4) are defined in the format Pyomo uses. The Pyomo solves the optimization problem through predefined solvers (such as GNU Linear Programming Kit) and the results are organized and analyzed as time-series through postprocessors. Primal results are reservoir storage and turbine release time-series. Post-processed results include hydroelectric generation and revenue.

The base-case FEHEM model has a database consisting of 45 years of historical hydrological data to represent hydrologic variability. Then, 45 years of historical hydrological data are perturbed to reflect the effects of selected two climate scenarios.

2.4. Storage–head relationship

For a plant with a large storage capacity, the water head varies depending on the reservoir levels. As storage increases, the height of the drop increases, and as storage decreases the height of the drop decreases. Depending on the topography of a reservoir site, there is a nonlinear relationship between water storage capacity, elevation, and energy storage. The gross head is the difference between the reservoir height and the tail water: $H = E_{\text{reservoir}} - E_{\text{tailwater}}$.

In the FEHEM model power plants, a polynomial curve is plotted between storage capacity and head to obtain storage–head relationship. Storage and elevation data are obtained from the volume–slope curves of the dams.

The coefficients in Equation (5) (θ, α, β, γ, and c) represent the polynomial parameters used by the model. Observed storage and elevation data are obtained from State Hydraulic Works (DSI). The index i represents the power plant, and H and S are head and storage, respectively.

$$H = \theta_i S^4 + \alpha_i S^3 + \beta_i S^2 + \gamma_i S + c_i \tag{5}$$

2.5. Penalties

In hydroeconomic modeling, water demands can be represented by functions of gross economic benefits over a given time period. In time periods with lower water deliveries than water demand, water scarcity costs are represented by penalty functions (Harou *et al.* 2009).

In the FEHEM model, water scarcity costs are represented by piecewise linear penalty functions for hydroelectric water demand. Penalties represent the loss of benefits from not producing energy. The x-axis of a penalty curve represents the amount of water supplied for hydroelectric and the y-axis represents the total cost (Figure 3). A linearly reversed graph would represent the hydroelectric benefit curve.

Hydroelectric generation is modeled with penalty curves in FEHEM, and power capacity, energy production, and revenue are calculated with a separate post-processor. A hydroelectric processor takes reservoir storage and turbine release data from the FEHEM output file and provides monthly time-series of power capacity, total monthly and annual energy production and revenue, amount of water spilled, and total turbine capacity used.

Equation (6) shows the hydroelectric utility function B at any given time t as a function of unit electricity price p, unit weight of water γ, flow rate Q, head as a function of storage $H(S)$, and efficiency e. The objective of FEHEM is to minimize

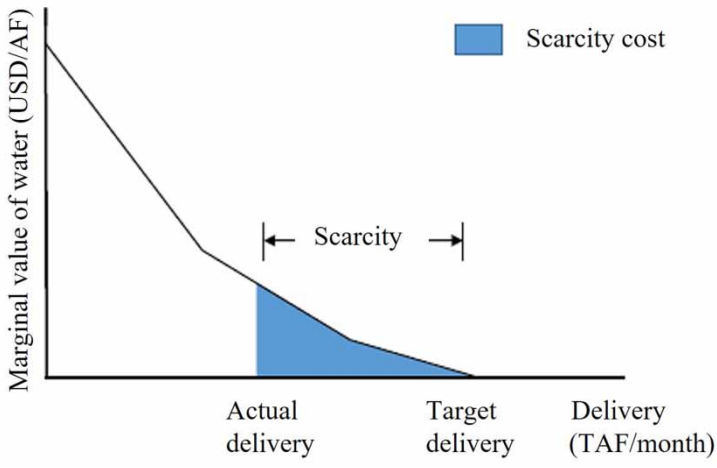

Figure 3 | Economic value of water (TAF, thousand acre-feet; AF, acre-feet) (Dogan 2015).

system-wide operating costs, which requires modeling hydroelectric benefits as penalty functions.

$$B_t = p_t \gamma Q_t H(S_t) e \tag{6}$$

Hydroelectric optimization requires the representation of two key inputs in addition to plant characteristics: these are reservoir flows and energy prices. It is assumed that hydroelectric operations do not affect energy prices. In a deterministic model, flow and price are assumed to be known with certainty. In these conditions, Equation (7) shows the total power (Watts) that can be produced as a function of water density, where ρ is the density (kg/m^3); acceleration due to gravity as g (m/s^2); plant efficiency = η (constant); H is the water head (m); and Q is the flow rate through the turbines (m^3/s). The product of these values gives the installed power in Watts.

$$\text{Power } = \rho.g.\eta.H.Q \tag{7}$$

If we multiply the power by the time, t (hours), in a given period, ΔT, it gives the energy production (kWh) (Equation (8)):

$$\text{Energy} = \int_0^T \rho g \eta H(t) Q(t) dt \tag{8}$$

Multiplying the amount of energy produced by the energy price, $p(t)$ ($/kWh) yields hydroelectric revenue ($) (Equation (9)).

$$\text{Revenue} = \int_0^T \rho g \eta H(t) Q(t) p(t) dt \tag{9}$$

For N power plants in a network, the total hydroelectric revenue from all plants and time steps (Equation (10)) can be formulated as follows:

$$\text{Total revenue} = \sum_i^N \sum_t^T g \eta_i H_{i,t} Q_{i,t} p \Delta t \tag{10}$$

For fixed head plants, the head H does not change over time T for a given plant i. However, in variable head plants with large storage capacity, H can be expressed in terms of water head in terms of storage, and this depends on two variables: turbined flow Q and stored flow S (Equation (11)).

$$\text{Total revenue} = \sum_i^N \sum_t^T \rho g \eta_i H(S)_{i,t} Q_{i,t} p \Delta t \tag{11}$$

2.6. Energy prices

Energy prices are the economic value of a unit of energy production in the energy market. The energy market consists of a system operator, scheduling coordinators, the energy exchange, public utility distribution companies, retail companies, and customers. In the energy exchange, the price for each day and each hour of the day is determined by automatic auction, while the lowest possible cost electricity is delivered to the interconnected system through distribution and retail companies to meet demand. In FEHEM, energy prices are obtained from EPIAS (Energy Exchange Istanbul-EXIST). These values are converted into monthly average energy prices and entered into the model.

2.7. Perturbed hydrology

In order to determine the impacts of climate change in the FEHEM model, 45 years of hydrological historical dataset is perturbed and the model is run under two scenarios with low and high carbon emissions. In these simulations, the current measurement values of Palu and Bagistas current observation stations, which will represent the flows of the Upper Euphrates

Basin, for1971–2016 were compared with the flows for 2071–2116 obtained from climate model simulations. Percentage differences between them according to months were determined. Climate scenarios reflect future hydrological variability. Figure 4 shows the monthly average historical inflows between 1970 and 2016 (historical) and perturbed inflows according to climate models ECHAM5 and CCSM3. Historical inflows show typical snow-fed river characteristics. Monthly values of the flows show that significant melting started in March and ended in June and July. Most peaks occur in April with 20–40% of the annual flow, while Karasu River's peak appears in May. The graphs show that slight increases occur mostly from November through March, while significant decreases are mostly from April through July.

In the low-emission ECHAM5 scenario, an average decrease of 50% is observed in April, May, and June when the flow increases under historical conditions. In December, January, and February, there is an average increase of 40% compared to historical hydrological data. According to the ECHAM5 model, the average flow carried by the rivers in the FEHEM region shows a record decrease of 61%. The January average shows an increase of 54%.

According to the high-emission CCSM3 scenario, the flow carried by the rivers in the FEHEM region will decrease by an average of 80% in spring. An increase of 30% is expected from January only. In the whole basin, the CCSM3 simulation predicts earlier timing of the annual peak discharges and lower peak season flows.

In both models, it is seen that the annual total flow amounts decrease significantly. Generally, the largest current losses occur in the April–July period. The increase in flows is spread over the January–March period. This can be explained by the fact that snowmelt in the FEHEM region occurs at an earlier time interval due to the increasing temperature with climate change. The reason for the decrease in the spring–summer period can be explained as the decrease in the total amount of precipitation. Generally, it is observed that the flow rates in the fall months do not change significantly. This can be explained by the fact that the Upper Euphrates Basin is located in a region where arid climate conditions prevail.

3. RESULTS AND DISCUSSION

3.1. Reservoir operations

Reservoirs are important water management tools. They store water when it is more abundant and release it when demand and energy unit prices are high. With the time shift in peak flows due to the possible effects of climate changes, and with snow

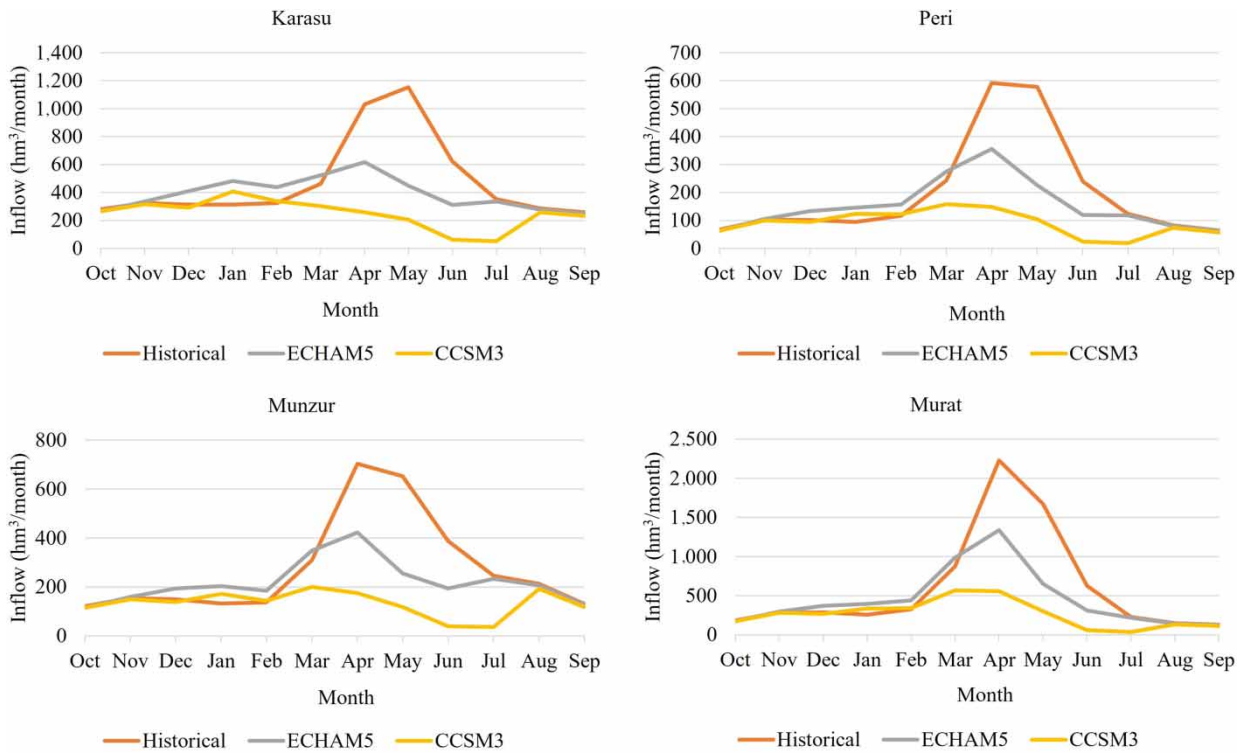

Figure 4 | Monthly average flow changes of river energy stages in climate scenarios.

melting earlier in spring under higher emission climate conditions, peak storage occurs earlier. Moreover, all climate scenarios show that the annual amount of storage in FEHEM basins will decrease. The largest annual average storage in the basin total is about 25.98 BCM with historical hydrology, which decreases to 24 BCM under the ECHAM5 scenario and 18 BCM under the CCSM3 scenario. According to the historical hydrology in Figure 5, the average annual minimum surface storage value of around 12 BCM will decrease to 8 BCM.

At all times, average annual surface water storage with perturbed hydrology is less than historical surface storage. According to the high-emission CCSM3 scenario, the loss in annual storage is around 30%. This reduction in the amount of surface storage is projected to reduce the reliability of storage with climate change, reducing system-wide hydroelectric capacities and reducing energy revenues.

3.2. Hydroelectric generation

FEHEM reservoirs generally store water in winter and spring. In other months, it is turbined because the unit energy price is higher and the energy demand is higher. Since the general operating principle of the model is to maximize total utility, there is generally a tendency to store in months when the unit price of energy is low, and a tendency to turbine in months when the unit price of energy is high to increase revenue. The average monthly electric generation in the FEHEM region is quite high in spring. Production decreases with decreasing flow in the summer and fall months. Low- and high-emission climate scenarios are shown in Figure 6. Accordingly, energy values decrease at very high rates in the months of high production and reach similar figures in almost every month of the year.

Figure 6 shows the basin-wide monthly modeled hydroelectric generation and revenue under historical and projected climate scenarios. In general, monthly production and revenue patterns do not differ significantly, with coinciding peaks and lows. However, energy generation and revenue significantly decrease with climate change, especially between March and August. In FEHEM basins, energy generation and revenue are higher in spring months under historical hydrology. When energy bars and revenue line is analyzed in Figure. 6, it is seen that energy bars exceed the revenue line in spring months. In other months, the revenue line is above the energy bars. This can be explained by the low unit price of energy in the spring months and the low total income relative to the energy produced. The average annual hydroelectric generation across the region is 9,481.88, 4,631.04, and 3,966.32 GWh per year with hydroelectric benefits of $619.69 million, $316.10 million, and $267.71 million for the historical, ECHAM5, and CCSM3 climate cases, respectively. The average annual reduction in hydroelectric generation is about 50%, corresponding to an annual revenue loss of about 300 million dollars. The annual reduction of about 5,000 GWh corresponds to about 7% of Turkey's average hydroelectric power generation

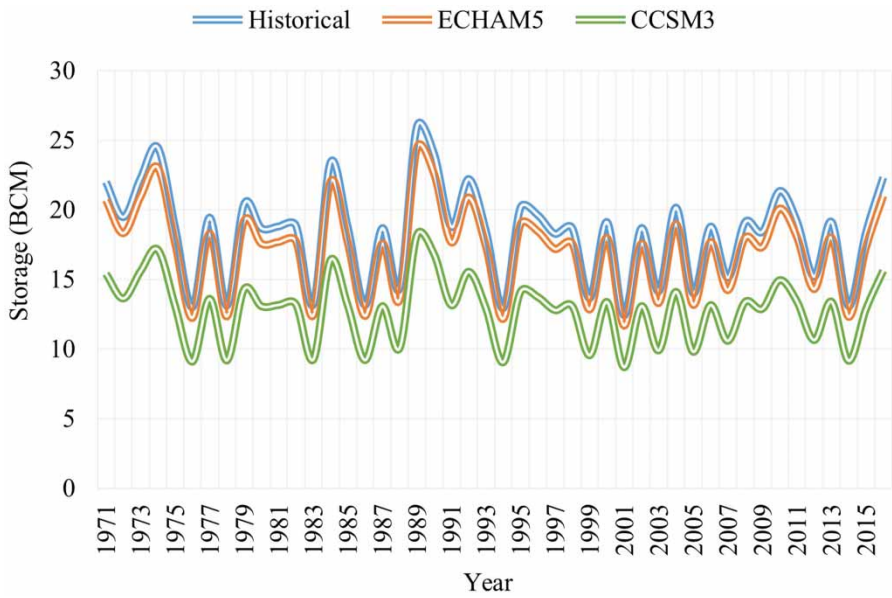

Figure 5 | FEHEM reservoirs monthly turbine discharge.

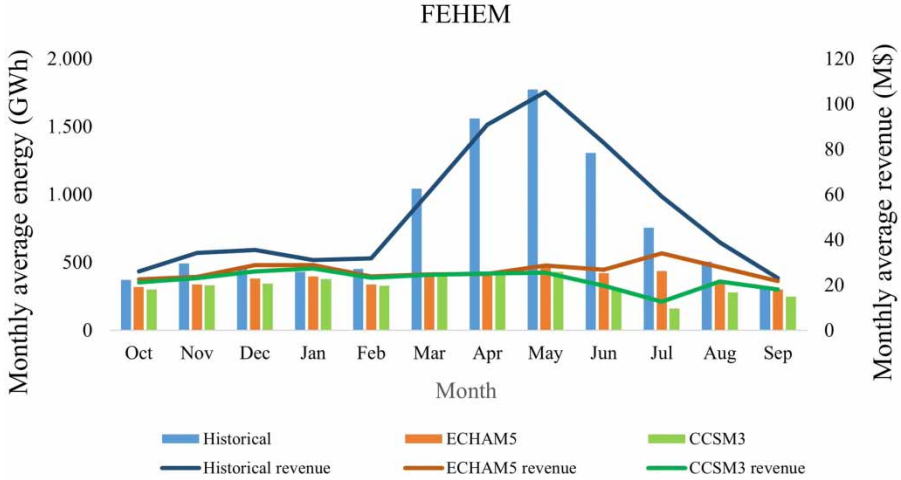

Figure 6 | FEHEM monthly average energy generation and revenue with modeled climate scenarios.

in 2021. When all climate scenarios are analyzed, it is seen that monthly average energy and income values drop significantly in the spring months.

Figure 6 shows that the monthly average of the power plants modeled under historical climatic conditions peaked in May with a production of 105.26 GWh. Although the highest production occurs in May, it drops to 28.66 GWh for ECHAM5 and 25.48 GWh for CCSM3 with climate changes. This reveals that approximately 75% of energy can be lost. In particular, peak production in the March–July period decreases to almost the same level as in other months. When the results are evaluated in terms of both climate scenarios, it will lead to a very serious energy loss by the end of the century.

Many of the FEHEM hydroelectric plants have large storage capacities; however, average annual hydroelectric generation and income are decreasing with global warming due to decreasing total precipitation and runoff. According to the model results described in Table 2, the biggest decline in hydroelectric generation is in the Peri Basin. Climate change has less impact on the Murat River, where the Asagikalekoy and Beyhan power plants are located. In addition, according to the results of both climate scenarios, there will be significant decreases in the Munzur and Karasu energy groups. The total energy production amount of the Munzur energy group will be lost by 55.6% compared to the low-emission scenario, while the Karasu energy group will experience a loss of 59.42% compared to the high-emission scenario. There will be a 50% loss of energy and income across the basin. The annual average energy reduction is 51.16% for the ECHAM5 climate scenario and 58.17% for CCSM3.

Climate scenarios show that there will be less water availability in FEHEM regions. Due to these expected dry climatic conditions, hydroelectric generation will decrease. Figure 7 shows production reliabilities of the Keban hydroelectric plant under hot and dry hydrological conditions with historical high (CCSM3) and low (ECHAM5) emissions. In all scenarios, the reliability of monthly average hydroelectric generation decreases at any probability level. In general, as hydroelectric generation increases, the differences in generation reliability become more pronounced. Even the spring production of the Keban Dam will be drastically reduced. The production of 1,000 GWh drops to 200 GWh under both scenarios. The production of

Table 2 | Regional hydroelectric revenues

	Energy (GWh/year)			Difference (%)	
Region	**Historical**	**ECHAM5**	**CCSM3**	**ECHAM5**	**CCSM3**
Murat Energy Group	2,039.6	1,147.5	880.1139	– 43.74	– 56.85
Peri Energy Group	1,555.0	590.3	573.2093	– 62.04	– 63.14
Munzur Energy Group	219.4	97.4	101.0756	– 55.61	– 53.93
Karasu Energy Group	429.1	205.5	174.1484	– 52.11	– 59.42
FEHEM	9,481.9	4,631.0	3,966.3	– 51.16	– 58.17

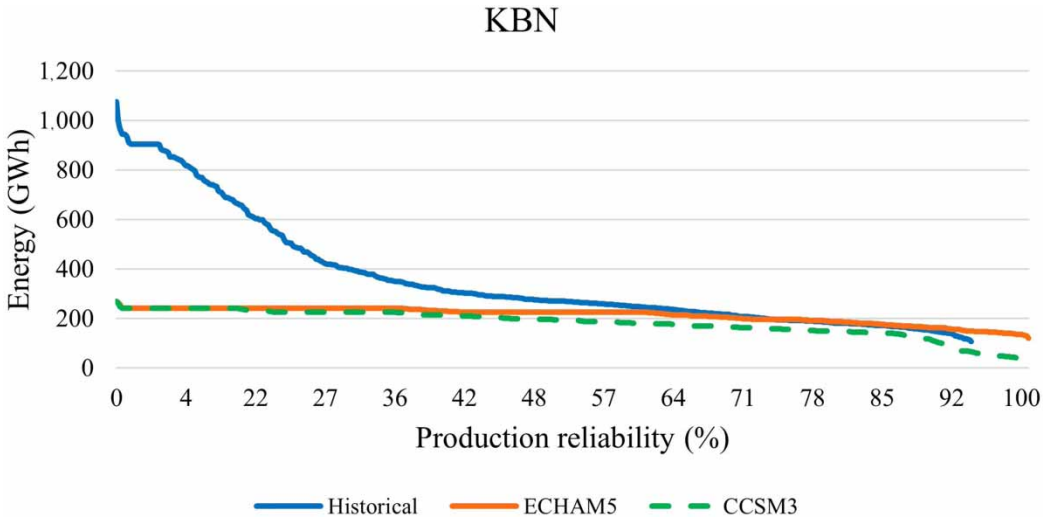

Figure 7 | Keban dam hydroelectric generation-exceedance probability curve.

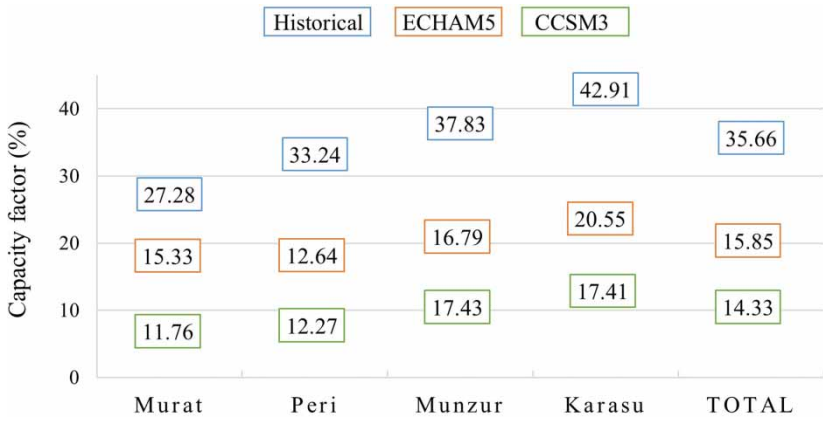

Figure 8 | Regional average turbine capacity utilization in historic and hot-dry climates.

1,000 GWh decreases to 200 GWh in both scenarios. As a result, the consistent and reliable energy output from the power plants (firm energy) will decrease significantly. When historical data are analyzed, it is seen that the production curve is not horizontal and has a trend from high to low values.

In the warmer and drier climate scenarios, the average turbine capacity utilization in the FEHEM region decreases by about 20% in the ECHAM5 climate scenario and by about 21% in the CCSM3 scenario (Figure 8). The highest capacity factor in the FEHEM region belongs to the Karasu Basin, while the lowest capacity factor belongs to the Murat Basin. Likewise, according to the ECHAM5 climate scenario, the highest capacity factor is observed for the Karasu Basin and the lowest for the Peri Basin. For the CCSM3 climate scenario, the highest capacity factor is projected to be in the Munzur Basin with 17.43%, while the lowest value is projected to be in the Murat Basin with 11.76%. It can be said that the capacity factors of low- and high-emission climate scenarios are close in the Peri and Munzur basins.

4. CONCLUSIONS

The aim is to simulate hydroelectric operations with the FEHEM model under different possible future climate conditions, in addition to historical climate conditions. For this purpose, two different possible future climate scenario conditions were integrated into the FEHEM model to determine the impact of global warming and climate change. The effects of drier climate

conditions on the Upper Euphrates Basin hydroelectric generation are investigated. CCSM3 represents the high carbon emission scenario and ECHAM5 represents the low carbon emission scenario.

The shift of spring snowmelt to early winter months will result in a decrease in spring flows and an increase in winter flows. This shift will directly affect reservoir operations and hydroelectric generation. According to the model results, the total reduction in reservoir inflows is calculated to be 52% for the high emission and about 23% for the low-emission climate model.

It can be said that the ECHAM5 climate model has less impact on the total energy production of the Murat River compared to other basins with a difference of −43.74%. The Murat River has dams with large storage capacities, and due to the operational flexibility provided by this capacity, it can be said that their impact on energy production is relatively low.

Likewise, according to the CCSM3 model, the least difference between the basins occurred in the Munzur basin (−53.93%).

Hydroelectric generation decreases in both climate scenarios due to less precipitation. Average annual hydroelectric power generation would decrease by 51.16% for the low-emission scenario and 58.17% for the high-emission scenario. Climate change is significantly reducing the production reliability of reservoirs in the FEHEM region. Decreases in flows will cause a decrease in the total energy of the dams as well as a decrease in their firm energy.

In parallel with the decrease in energy production, energy revenue also decreases. An average annual loss of hydroelectric revenue of USD303.59 million is expected for the low-emission scenario and USD351.98 million for the high-emission scenario.

While the average turbine capacity utilization across the basin is 36.6% under normal conditions, it decreases to 16.8% under the low-emission climate scenario and 14.33% under the high-emission climate scenario.

The FEHEM model stored an average of 21 BCM of water per year in reservoir storage operations. While this value reached 26 BCM in some years, there were also years when it decreased to 12 BCM. In the expected climate scenarios, the highest storage value was 24.41 BCM and the lowest storage value was 9.06 BCM. This shows that global warming and climate change will cause a decrease of around 30% in storage.

Changes in the timing and magnitude of water availability with possible climate change will vitally alter reservoir operations. Changing flow conditions under climate change increase levels of winter storage; however, summer and fall storage falls below the historical average. As storage capacity increases, with greater operational flexibility, facilities can better adapt to changing climates. However, small storage capacity facilities have little room to make operational adjustments and are therefore less adaptable.

AUTHORS CONTRIBUTIONS

A.A. and M.C.T. analyzed the data and wrote the paper. M.S.D. performed research conceptualization and methodology, supervised the work, and reviewed and edited the manuscript.

DATA AVAILABILITY STATEMENT

Data cannot be made publicly available; readers should contact the corresponding author for details.

CONFLICT OF INTEREST

The authors declare there is no conflict.

REFERENCES

Auffhammer, M. 2018 Quantifying economic damages from climate change. *Journal of Economic Perspectives* **32** (4), 33–52. doi: 10.1257/jep.32.4.33.

Aytac, A., Tuna, M. C. & Dogan, M. S. 2023 Development of Upper Euphrates Basin hydro-economic model and hydropower generation optimization. *Journal of Water and Climate Change* **14** (9), 3385. doi: 10.2166/wcc.2023.377.

Bozkurt, D. 2013 *Climate Change Impacts on the Hydrology of the Euphrates-Tigris Basin*. PhD Thesis, Istanbul Technical University.

Collins, W. D., Bitz, C. M., Blackmon, M. L., Bonan, G. B., Bretherton, C. S., Carton, J. A., Chang, P., Doney, S. C., Hack, J. J., Henderson, T. B., Kiehl, J. T., Large, W. G., McKenna, D. S., Santer, B. D. & Richard, D. S. 2006 The community climate system model version 3 (CCSM3). *Journal of Climate* **19** (11), 2122–2143. https://doi.org/10.1175/JCLI3761.1.

Davijani, M. H., Banihabib, M. E., Anvar, A. N. & Hashemi, S. R. 2016 Optimization model for the allocation of water resources based on the maximization of employment in the agriculture and industry sectors. *Journal of Hydrology* **533**, 430–438.

Di Piazza, A., Di Piazza, M. C., La Tona, G. & Luna, M. 2021 An artificial neural network-based forecasting model of energy-related time series for electrical grid management. *Mathematics and Computers in Simulation (MATCOM)* **184** (C), 294–305. Elsevier.

Dogan, M. S. 2015 *Integrated Water Operations in California: Hydropower, Overdraft, and Climate Change. Master of Science*, University of California Davis, Office of Graduate Studies

Dogan, M. S., Fefer, M. A., Herman, J. D., Hart, Q. J., Merz, J. R., Medell__n-Azuara, J. & Lund, J. R. 2018 An open-source Python implementation of California's hydroeconomic optimization model. *Environmental Modelling & Software* **108**, 8–13. doi:10.1016/j.envsoft.2018.07.002.

Dogan, M., Lund, J. & Azuara, J. 2021 Hybrid Linear and Nonlinear Programming Model for Hydropower Reservoir Optimization. *Journal of Water Resources Planning and Management* **147** (3). DOI:10.1061/%28ASCE%29WR.1943-5452.0001353.

Draper, A. J., Jenkins, M. W., Kirby, K. W., Lund, J. R. & Howitt, R. E. 2003 Economic- engineering optimization for California water management. *Journal of Water Resources Planning and Management* **129** (3), 155–164. http://doi.org/10.1061/(ASCE)0733-9496(2003)129:3(155).

Dufresne, J., Foujols, M., Denvil, S., Caubel, A., Marti, O., Aumont, O., Balkanski, Y., Bekki, S., Bellenger, H., Benshila, R., Bony, S., Bopp, L., Braconnot, P., Brockmann, P., Cadule, P., Cheruy, F., Codron, F., Cozic, A., Cugnet, D., de Noblet, N., Duvel, J. P., Ethé, C., Fairhead, L., Fichefet, T., Flavoni, S., Friedlingstein, P., Grandpeix, J. Y., Guez, L., Guilyardi, E., Hauglustaine, D., Hourdin, F., Idelkadi, A., Ghattas, J., Joussaume, S., Kageyama, M., Krinner, G., Labetoulle, S., Lahellec, A., Lefebvre, M. P., Lefevre, F., Levy, C., Li, Z. X., Lloyd, J., Lott, F., Madec, G., Mancip, M., Marchand, M., Masson, S., Meurdesoif, Y., Mignot, J., Musat, I., Parouty, S., Polcher, J., Rio, C., Schulz, M., Swingedouw, D., Szopa, S., Talandier, C., Terray, P., Viovy, N. & Vuichard, N. 2013 Climate change projections using the IPSL-CM5 Earth System Model: From CMIP3 to CMIP5. *Climate Dynamics* **40**, 2123–2165. https://doi.org/10.1007/s00382-012-1636-1.

Eamen, L., Brouwer, R. & Razavi, S. 2021 Integrated modelling to assess the impacts of water stress in a transboundary River Basin: Bridging local-scale water resource operations to a River Basin Economy. *Science of The Total Environment* **800**, 149543.

Farjad, B., Gupta, A., Razavi, S., Faramarzi, M. & Marceau, D. 2017 An integrated modelling system to predict hydrological processes under climate and land-use/cover change scenarios. *Water* **9** (10), 767.

Feng, Y., Zhou, J., Mo, L., Yuan, Z., Zhang, P., Wu, J., Wang, C. & Wang, Y. 2018 Long-term hydropower generation of cascade reservoirs under future climate changes in Jinsha river in southwest China. *Water* **10** (2), 235. https://doi.org/10.3390/w10020235.

Galavi, H. & Mirzaei, M. 2020 Analyzing uncertainty drivers of climate change impact studies in tropical and arid climates. *Water Resources Management* **34**, 2097–2109. https://doi.org/10.1007/s11269-020-02553-0.

Galavi, H., Mirzaei, M., Yu, B. & Lee, J. 2023 Bootstrapped ensemble and reliability ensemble averaging approaches for integrated uncertainty analysis of streamflow projections. *Stochastic Environmental Research and Risk Assessment* **37**, 1213–1227. https://doi.org/10.1007/s00477-022-02337-5.

Garrido-Perez, J. M., Barriopedro, D., García-Herrera, R. & Ordóñez, C. 2021 Impact of climate change on Spanish electricity demand. *Climatic Change* **165** (3), 1–18.

Hagemann, S., Chen, C., Clark, D. B., Folwell, S., Gosling, S. N., Haddeland, I., Hanasaki, N., Heinke, J., Ludwig, F., Voss, F. & Wiltshire, A. J. 2013 Climate change impact on available water resources obtained using multiple global climate and hydrology models. *Earth System Dynamics* **4**, 129–144. https://doi.org/10.5194/esd-4-129-2013.

Harou, J. J., Pulido-Velázquez, M., Rosenberg, D. E., Medellín-Azuara, J., Lund, J. R. & Howitt, R. E. 2009 Hydroeconomic models: Concepts, design, applications, and future prospects. *Journal of Hydrology* **375**, 627–643.

Hart, W. E., Laird, C. D., Watson, J.-P., Woodru_, D. L., Hackebeil, G. A., Nicholson, B. L. & Siirola, J. D. 2017 *Pyomo Optimization Modeling in Python*, Vol. 67. Springer International Publishing, Cham. doi:10.1007/978-3-319-58821-6.

Jakimavičius, D., Adžgauskas, G., Šarauskienė, D. & Kriaučiūnienė, J. 2020 Climate change impact on hydropower resources in gauged and ungauged Lithuanian river catchments. *Water* **12** (11), 3265. https://doi.org/10.3390/w12113265.

Morid, R., Shimatani, Y. & Sato, T. 2019 Impact assessment of climate change on environmental flow component and water temperature – Kikuchi River. *Journal of Ecohydraulics* **4** (2), 88–105.

Roeckner, E., Brokopf, R., Esch, M., Giorgetta, M., Hagemann, S., Kornblueh, L., Manzini, E., Schlese, U. & Schulzweida, U. 2004 *The Atmospheric General Circulation Model ECHAM5. Part II: Sensitivity of Simulated Climate to Horizontal and Vertical Resolution*. MPI-Report No. 354, MPI für Meteorologie, Hamburg, 55 pp

Russel, G. L., Gornitz, V. & Miller, J. R. 2000 Regional sea-level changes projected by the NASA/GISS atmosphere-ocean model. *Climate Dynamics* **16**, 789–797.

Tian, H., Lu, C., Pan, S., Yang, J., Miao, R., Ren, W., Yu, Q., Fu, B., Jin, F. F., Lu, Y. & Melillo, J. 2018 Optimizing resource use efficiencies in the food–energy–water nexus for sustainable agriculture: From conceptual model to decision support system. *Current Opinion in Environment Sustainability* **33**, 104–113.

Sarker, S. 2020 I*nvestigating Topologic and Geometric Properties of Synthetic and Natural River Networks under Changing Climate 2021*. Electronic Theses and Dissertations, 2020-965. Available from: https://stars.library.ucf.edu/etd2020/965

Solomon, S., Qin, D., Manning, M., Marquis, M., Averyt, K., Tignor, M. M. B., Miller Jr., H. L. & Chen, Z. 2007 *Climate Change 2007: The Physical Science Basis*. Cambridge University Press, Cambridge.

Xu, Z., Sheykhahmad, F. R., Ghadimi, N. & Razmjooy, N. 2020 Computer-aided diagnosis of skin cancer based on soft computing techniques. *Open Medicine* **15** (1), 860–871.

Ye, H., Jin, G. & Fei, W. 2020 High step-up interleaved dc/dc converter with high efficiency. *Energy Source A: Recovery, Utilization, and Environmental Effects* 1–20. doi: 10.1080/15567036.2020.1716111.

Yu, D., Zhang, T., He, G., Nojavan, S., Jermsittiparsert, K. & Ghadimi, N. 2020 Energy management of wind-PV-storage-grid based large electricity consumer using robust optimization technique. *Journal of Energy Storage* **27**, 101054.

Zaman, M. R., Morid, S. & Delavar, M. 2016 Evaluating climate adaptation strategies on agricultural production in the Siminehrud catchment and inflow into Lake Urmia, Iran using SWAT within an OECD framework. *Agricultural Systems* **147**, 98–110.

Zhang, D. & Guo, P. 2016 Integrated agriculture water management optimization model for water saving potential analysis. *Agricultural Water Management* **170**, 5–19.

First received 16 September 2023; accepted in revised form 15 January 2024. Available online 29 January 2024